Valence band structure of the icosahedral Ag-In-Yb quasicrystal

H. R. Sharma,[1,*] G. Simutis,[1] V. R. Dhanak,[1] P. J. Nugent,[1] C. Cui,[2] M. Shimoda,[3] R. McGrath,[1] A. P. Tsai,[2,3] and Y. Ishii[4]
[1]*Surface Science Research Centre and Department of Physics, The University of Liverpool, Liverpool L69 3BX, United Kingdom*
[2]*Institute of Multidisciplinary Research for Advanced Materials, Tohoku University, Sendai 980-8577, Japan*
[3]*National Institute for Materials Science, 1-2-1 Sengen, Tsukuba, Ibaraki 305-0047, Japan*
[4]*Department of Physics, Chuo University, Kasuga, Tokyo 112-8551, Japan*
(Received 8 January 2010; revised manuscript received 23 February 2010; published 18 March 2010)

The valence band structure of the icosahedral (*i*) Ag-In-Yb quasicrystal, which is isostructural to the binary *i*-Cd-Yb system, is investigated by ultraviolet photoemission spectroscopy (UPS). Experimental results are compared with electronic-structure calculations of a cubic approximant of the same phase. UPS spectra from the fivefold, threefold, and twofold *i*-Ag-In-Yb surfaces reveal that the valence band near to the Fermi level is dominated by Yb 4*f*-derived states, in agreement with calculations. The spectra also exhibit peaks which are surface core level shifted, caused by changes in the electronic structure in surface layers. Calculations yield a pseudogap in the density of states due to a hybridization of the Yb 5*d* band with the Ag 5*p* and In 5*p* bands. Both experimental and calculated band features are very similar to those of Cd-Yb. The modification of the band structure after surface treatment by sputtering and by oxidation is also studied. Additionally, the work function of *i*-Ag-In-Yb measured from the width of UPS spectrum is found to be almost unaffected by surface orientation, but increases after sputtering or oxidation.

DOI: 10.1103/PhysRevB.81.104205 PACS number(s): 79.60.−i, 71.23.Ft, 82.80.Ej

I. INTRODUCTION

The discovery of the stable binary icosahedral (*i*) Cd-Yb quasicrystal[1] was a major advance in the field. Consisting of two elements, it is simpler than ternary icosahedral quasicrystals for theoretical determination of atomic structure and physical properties. This together with the chemical order and structural perfection of *i*-Cd-Yb have led to a full structural solution of an icosahedral quasicrystal.[2] The structure of the system can be described as an aperiodic arrangement of rhombic triacontahedral (RTH) clusters which consist of five successive atomic shells. The RTH clusters cover 93.8% of the total atoms in the crystal. The remaining atoms in the interstices (called glue atoms) can be precisely specified using acute and obtuse rhombohedra.[2]

Electronic-structure calculations of the 1/1 approximant of *i*-Cd-Yb (Ref. 3) have provided a new insight on the origin of the pseudogap in the density of states at the Fermi level, which is the most universal feature of quasicrystals.[4] It was believed that the pseudogap is due to the Hume-Rothery mechanism combined with *sp-d* hybridization (see Ref. 5 for a review). However, Ishii and Fujiwara[3] showed that the pseudogap in *i*-Cd-Yb is determined primarily by a hybridization of the Yb 5*d* band with the Cd 5*p* band (*p-d* hybridization), rather than the Hume-Rothery mechanism. This conclusion was later supported by photoemission experiments.[6]

Furthermore, the lower degree of chemical disorder in *i*-Cd-Yb compared with ternary quasicrystal phases presents an opportunity to study the inherent effect of aperiodic ordering on physical properties, i.e., independent of chemical disorder. Transport properties of the system are notably different from those of Al-based ternary quasicrystals.[7–9] These include higher electrical conductivity, very large electronic specific-heat coefficients, low Debye temperatures and high magnetoresistance.[7–9]

Despite progress in bulk studies, knowledge of the surface properties of the binary *i*-Cd-Yb phase is very limited compared to Al-based ternary quasicrystals, where many studies have been conducted and several new phenomena discovered.[10,11] The main problem is that *i*-Cd-Yb is not suitable for surface preparation in ultrahigh vacuum (UHV) conditions because the high vapor pressure of Cd leads to evaporation upon heat treatment. This difficulty can be overcome by replacing Cd by Ag and In, the adjacent elements to Cd in the periodic table. The replacement of Cd by 50% Ag and 50% In maintains the valence electron to atom ratio of 2.0, which is a necessary condition for the formation of this phase.[12,13] As Ag and In are both stable in UHV, surface studies of this icosahedral quasicrystal are therefore possible.[14,15] It is also of interest to learn whether the presence of Ag and In makes the physical properties of this phase different from those of *i*-Cd-Yb. So far only a few studies addressed this issue. Transport properties of Ag-In-Yb phases are found to be very similar to those of Cd-Yb.[16]

In this paper, we compare the valence band structure of the *i*-Ag-In-Yb quasicrystal studied by ultraviolet photoemission spectroscopy (UPS) with the results of electronic-structure calculations of a cubic approximant of the same system. Results are also compared with previous photoemission studies of *i*-Cd-Yb (Ref. 17) and calculations of Cd-Yb approximant.[3] The influence of the surface orientation on the valence band is studied using the fivefold, threefold, and twofold surfaces and the effects of surface modification by sputtering, annealing, and oxidation are also investigated. We also compare UPS results from these surfaces with bulk Ag, In, and Yb. In addition, the change in work function after different surface treatments is investigated.

II. EXPERIMENTAL DETAILS

The single grain *i*-$Ag_{42}In_{42}Yb_{16}$ sample was grown by the Bridgman method[18] and cut perpendicular to the fivefold,

threefold, and twofold axes. Each sample was then polished using successively fines grades of diamond paste down to 0.25 μm. Subsequently, the surfaces were prepared in a UHV chamber with base pressure of 2×10^{-10} mbar by repeated cycles of Ar^+ sputtering at 2 keV for 15 min (10 μA ion current) and annealing at 715 K for 1 h. The pressure during annealing remained below 5×10^{-10} mbar. The cleanliness and composition of the surfaces was assessed by x-ray photoemission spectroscopy (XPS) with Al $K\alpha$ radiation ($h\nu$=1486.6 eV) using a PSP vacuum technology hemispherical electron-energy analyzer.

For bulk metal studies, foils of 99.9% pure Yb and In and a single crystal of Ag with (111)-surface orientation were used. Each sample was cleaned by Ar^+ sputtering. The Yb sample was difficult to prepare: a trace of oxygen was still detectable by XPS after many cycles of sputtering. However, the presence of this tiny amount of oxygen did not influence the position of the Yb 4*d* and Yb 4*f* bands.

UPS measurements were performed with nonmonochromatized He I radiation (21.2 eV) at normal emission. Helium pressure in the analysis chamber was kept constant (3×10^{-8} mbar) for all sets of experiments. The Fermi level was determined by measuring UPS spectra from a Ta strip connected to the sample. The midpoint of the Fermi edge in the spectra is taken as the position of the Fermi level. Oxidation was carried out in vacuum by introducing 99.6% pure oxygen gas through a leak valve. All UPS/XPS measurements and oxygen exposures were performed at room temperature. The energy resolution for UPS is about 100 meV for the employed pass energy of the analyzer 5–10 eV.

III. DETAILS OF THE ELECTRONIC STRUCTURE CALCULATIONS

The electronic structure of the 1/1 cubic approximant of *i*-Ag-In-Yb is studied by a conventional band calculation method. The structure of the cubic approximant is composed of icosahedral clusters on the vertices and the body center of a cubic unit cell.[1] The core of the cluster is an atomic shell of nonicosahedral symmetry, presumably of tetrahedral shape. The second and third atomic shells are a dodecahedron of 20 atoms and an icosahedron of 12 atoms, respectively. The fourth shell is an icosidodecahedron obtained by placing 30 atoms on the edge of the third shell. A few more atoms are placed between the clusters and can be interpreted as forming a triacontahedral fifth shell interpenetrating with the neighboring cluster.[2]

Goméz[19] has studied chemical ordering in the Ag-In-Yb cubic approximant. The innermost core and the fourth shell consist of In atoms whereas the second one consists of mainly Ag. The third shell is occupied by Yb atoms as in the case of Cd-Yb. We assume a chemically ordered structural model for the cubic approximant according to these observations. The alloy composition of the model is $Ag_{39}In_{47}Yb_{14}$ atomic %. The ratio of the number of Ag, In, and Yb atoms in the unit cell is 32:40:12. Starting from atomic positions for cubic Cd_6Yb, we relaxed the atoms to their optimal positions under the symmetry constraint that the space group is $I23$.[20] The lattice constant is chosen to be 15.4118 Å as reported by Goméz.[19] Structural relaxation was done with the *ab initio* total-energy and molecular-dynamics program Vienna *ab initio* simulation package[21,22] with the projected-augmented wave method.[23] The wave functions are expanded with a plane-wave basis set up to a kinetic-energy cutoff of 300 eV. The Brillouin zone is sampled by $3\times3\times3$ Monkhorst-Pack grids (four irreducible *k* points). Optimized atomic positions are given in Table I.

TABLE I. Atomic positions in the unit of the lattice constant *a* in the unit cell of the cubic Ag-In-Yb approximant obtained after structural relaxation as described in the text (space group: $I23$, a = 15.4118 Å).

Element	Wyckoff position (Ref. 24)	*x*	*y*	*z*
In	24f	0.198382	0.115382	0.332627
In	24f	0.799987	0.886377	0.657883
Ag	24f	0.997116	0.403259	0.355339
Ag	24f	0.998121	0.238177	0.092279
In	12e	0.203735	0.000000	0.500000
In	12d	0.402833	0.000000	0.000000
Ag	8c	0.151568	0.151568	0.151568
Ag	8c	0.828002	0.828002	0.828002
In	8c	0.430230	0.430230	0.430230
Yb	24f	0.997586	0.183967	0.295794

The electronic density of states (DOS) is calculated with the tight-binding linear muffin-tin orbitals method in the atomic-sphere approximation.[25] Calculations are based on the local-density approximation in the density-functional theory. We do not consider the spin-orbit interaction in self-consistent calculations but we estimate the splitting by using the Yb 4*f* wave function in the atomic sphere as 1.34 eV.

IV. RESULTS AND DISCUSSION

The structure and chemical compositions of the fivefold *i*-Ag-In-Yb surface after sputtering and annealing have been characterized by various surface-science techniques.[14,15] Analysis based on scanning tunneling microscopy (STM) results from the fivefold *i*-Ag-In-Yb surface and the bulk structural model of the isostructural *i*-Cd-Yb reveals that after annealing the surface forms at bulk positions which are dense and intersect the center of rhombic triacontahedral clusters.[15] The chemical composition of the surface after annealing is very similar to that of the bulk.[14] However, sputtering preferentially removes In and Yb resulting in Ag enrichment in the surface region. The resulting composition of $Ag_{71}In_{24}Yb_5$ (Ref. 14) is confirmed in the present study by XPS intensity analysis. No low-energy electron diffraction (LEED) or reflection high-energy electron diffraction[14] patterns were observed from the surface after sputtering, revealing a disordered surface structure.

With this understanding of the surface structure and chemical composition, we investigate the valence band structure of the system. Figure 1 shows a UPS spectrum taken

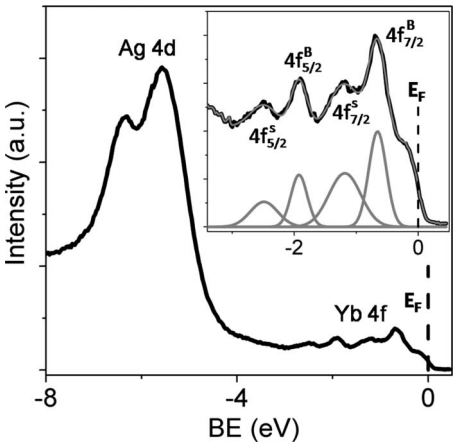

FIG. 1. Valence band spectrum of the fivefold *i*-Ag-In-Yb surface after annealing taken with He-I radiation. Inset shows a closeup near the Fermi level. Gray curves correspond to the results of a fit as described in the text. The Fermi level E_F is marked by a dotted line.

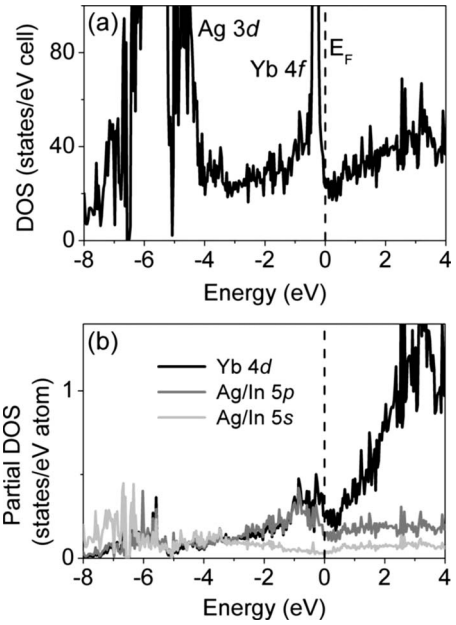

FIG. 2. (a) Total density of states of 1/1 cubic approximant of *i*-Ag-In-Yb calculated with the tight-binding linear muffin-tin orbitals method. (b) Partial density of states for Yb 4*d* (black), Ag/In 5*p* (gray), and Ag/In 5*s* (light gray). Vertical dotted lines mark the Fermi level.

from the fivefold surface after annealing. The spectrum consists of two strong peaks at around 5.6 and 6.3 eV below the Fermi level (E_F) in addition to low intensity peaks near E_F. A closeup near E_F is shown in Fig. 1 inset. In this region, two peaks are observed at 0.68 and 1.90 eV, each of which is accompanied by a weak peak in the vicinity. The peak positions were determined by fitting the data using Gaussian functions for peaks and a linear background. The results of the fit are given in Fig. 1 inset. All peak positions given in this report are within an error of ± 0.1 eV.

By comparing the valence band spectrum of *i*-Ag-In-Yb with that of pure Ag, In, and Yb, we attribute the peaks at 5.6 and 6.3 eV to the Ag 4*d* states, and the peaks near E_F to the Yb 4*f*-derived states (see below). We identify peaks at 0.68 and 1.90 eV as the spin-orbit doublets of the Yb 4*f* states, i.e., $4f_{7/2}$ and $4f_{5/2}$. The other two peaks in the vicinity can be identified as due to the Yb 4*f* states but shifted to higher binding energy (BE) due to changes in electronic structure in the surface layers, called surface core-level shift effect.[26–30] The surface-induced doublets will be labeled as $4f^S_{7/2}$ and $4f^S_{5/2}$ and the parent doublets as $4f^B_{7/2}$ and $4f^B_{5/2}$. The measured separation of the bulk doublets $\Delta E_B = \mathrm{BE}_{4f^B_{5/2}} - \mathrm{BE}_{4f^B_{7/2}}$ and the surface doublets $\Delta E_S = \mathrm{BE}_{4f^S_{5/2}} - \mathrm{BE}_{4f^S_{7/2}}$ is similar to the atomic spin-orbit energy of 1.27 eV. This is also close to the value estimated from the Yb 4*f* wave function in the atomic sphere (Sec. III).

The experimental valence band features are found to be in good agreement with electronic-structure calculations. Figure 2(a) shows the calculated DOS for the 1/1 approximant of *i*-Ag-In-Yb. As observed experimentally, the Ag 4*d*-derived band appears at around 4–6 eV. Calculations yield a narrow 4*f* band of Yb, which is fully occupied, at 0.3 eV below the Fermi energy. Due to the well-known self-interaction error in the local-density approximation,[31] which is considerably large for localized 4*f* states, the Yb 4*f* band does not appear at a position expected from experiments. It is positioned at lower binding energy compared to the experimental observation. Nevertheless, the Yb 4*f* state in the calculation is fully occupied as observed experimentally. Figure 2(b) shows the partial DOS for Yb 4*d*, Ag/In 5*p*, and Ag/In 5*s*. The Yb 4*f* component is not considered in this figure. A large value in the DOS above the Fermi energy is due to the contribution from the Yb 5*d* band. The Yb 5*d* also has certain amplitude just below the Fermi level, which is similar to that of Ag/In 5*p*. However, the contribution from the Ag/In 5*s* states is minimal across the Fermi level. Therefore, we conclude that the dip in the DOS (pseudogap), which is located slightly above the Fermi level, is due to a hybridization of the Yb 5*d* band with the Ag/In 5*p* band, as in Cd-Yb.[3]

A comparison of UPS spectra from *i*-Ag-In-Yb and pure Ag, In, and Yb is given in Fig. 3. The binding energies of the Yb 4*f* doublets for *i*-Ag-In-Yb and pure Yb derived from these spectra are given in Table II. Pure Yb, such as *i*-Ag-In-Yb, exhibits four peaks near E_F. Compared to these peaks, Yb peaks in *i*-Ag-In-Yb are shifted to lower binding energy by 0.50 eV. The position and relative intensity of the peaks enables us to unambiguously identify the Yb 4*f*-derived peaks in *i*-Ag-In-Yb. Similarly, the peaks at 5.6 and 6.3 eV in the *i*-Ag-In-Yb spectrum show a slight shift to higher binding energy compared to the 4*d* band of pure Ag which consists of peaks at 4.9, 5.5, and 6.0 eV and shoulders at 3.1, 4.3, 5.0, and 7.0 eV (Fig. 3). The observed peaks and shoulders in pure Ag are consistent with previous results[32] except for the shoulder at 5.0 eV. This shoulder is routinely observed in the sputtered surface but disappears after annealing. Pure In does not show any peaks in the measured energy range.

The shift of the Yb 4*f*-derived peaks to lower binding energy and the Ag 4*d*-derived peaks to higher binding energy in *i*-Ag-In-Yb can be explained if charge transfer occurs

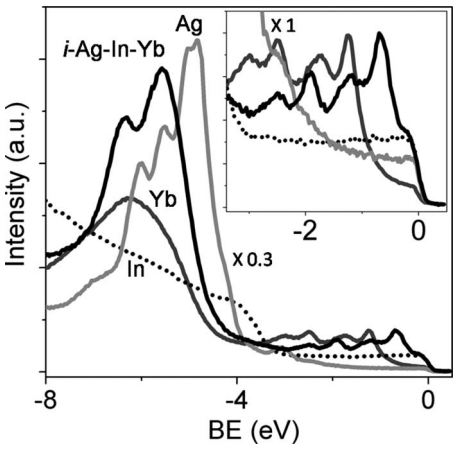

FIG. 3. He-I valence band spectra of the fivefold *i*-Ag-In-Yb surface and pure Ag, In, and Yb surfaces. Intensity of each spectrum is subtracted from background intensity above the Fermi level. Intensity of Ag spectrum is scaled by a factor of 0.3. The broad peak at around 6 eV in Yb spectrum is due to oxygen 2*p* states. Inset shows a closeup near the Fermi level.

from Ag to Yb in the alloy. XPS results from *i*-Ag-In-Yb (not shown) reveal core-level shifts of the Yb 4*d* and Ag 3*d* states in opposite directions, consistent with this hypothesis. However, no chemical shift is observed in the In core levels in *i*-Ag-In-Yb.

A noticeable feature is that the surface-induced Yb 4*f* peaks are observed in *i*-Ag-In-Yb as in pure Yb and its periodic compounds.[26–30] These peaks disappear after a slight contamination of the surface by the residual gases in the chamber, further agreeing with their surface origin. The existence of the surface core-level shift implies that the electronic structure at the surface differs from the bulk electronic structure. The measured surface core-level shift in *i*-Ag-In-Yb is ~0.50 eV, which is similar to the value for pure Yb (see Table II). It is also close to the theoretical value of 0.53 eV obtained for divalent Yb,[26] but slightly less than the experimental value of 0.60 eV observed in polycrystalline Yb by Gerken *et al.*[27] This is probably due to the fact that Gerken *et al.* used a surface prepared by evaporation on a substrate in contrast to the present surface prepared by sputtering a foil. We note that the surface core-level shift for a single-crystal surface is expected to be lower compared to a polycrystalline sample. For example, the close-packed Yb(111) surface shows a shift of 0.45 eV.[29] The surface core-level shift for various Yb compounds lie in a range of 0.52–0.94 eV.[28]

Tamura *et al.*[17] studied the valence band structure of *i*-Cd-Yb quasicrystal by photoemission spectroscopy and identified both bulk $4f^B_{7/2}$ and $4f^B_{5/2}$ peaks and surface-induced $4f^S_{7/2}$ and $4f^S_{5/2}$ peaks (see Table II). The bulk peaks are at similar positions as in *i*-Ag-In-Yb. However, the surface-shifted peaks are found at different positions. The surface core-level shift in *i*-Cd-Yb is 0.36 eV, which is much less than the value in *i*-Ag-In-Yb. Furthermore, the $4f^S_{7/2}$ and $4f^S_{5/2}$ peaks are much weaker in *i*-Cd-Yb. This could be because the two surfaces were prepared by different methods. In contrast to the sputter-annealing method used in the current study, the *i*-Cd-Yb surface was prepared by fracturing the sample *in situ*. The detail of the fractured surface, in terms of structure, morphology, and composition, was not known. The authors speculated, based on the results of the fractured *i*-Al-Pd-Mn surface,[33] that the RTH clusters persist at the surface.[17] In this situation, the chemical environment of surface Yb atoms will be similar to that of bulk Yb atoms. In contrast to this picture, the RTH clusters in *i*-Ag-In-Yb are truncated at the surface which is atomically flat.[15] This yields a different environment for Yb atoms at the surface than in the bulk. We note that the influence of surface preparation methods on electronic properties has also been observed in Al-based quasicrystals.[34]

The valence band is modified after the surface is sputtered or oxidized. Figure 4 compares UPS spectra from the fivefold *i*-Ag-In-Yb surface after sputtering, annealing, and oxidation. As explained earlier, sputtering preferentially removes Yb and In and the surface becomes Ag rich. The change in the chemical composition after sputtering is reflected in the valence band structure. The Yb 4*f*-derived peaks completely disappear after sputtering, probably due to the depletion of Yb. The Ag 4*d*-derived peaks are also shifted to lower binding energy and their relative intensity increases as expected from the altered composition of the sputtered surface. For oxidation studies, the surface was freshly prepared (sputter annealed) and exposed to 10 L of oxygen. UPS spectra from the surface after oxidation indicates that a shoulder develops at around 4.5 eV and that the intensity at higher binding energies increases. These changes can be explained by a shift of the Yb 4*f* band to higher binding energy. UPS spectra from pure Yb after oxidation confirm a shift of the 4*f* band to higher binding energy, consistent with previous results.[35] The shoulder marked by + sign in Fig. 4 is considered to be the contribution from the Yb 4*f* band shifted to higher binding energy after oxidation. The determination of the precise position of the band is not possible due to the overlap with the peak at higher energy. A

TABLE II. Binding energy (BE) in electron volt for bulk ($f^B_{7/2}$,$f^B_{5/2}$) and surface ($f^S_{7/2}$,$f^S_{5/2}$) doublets of Yb 4*f* states in *i*-Ag-In-Yb and pure Yb deduced from UPS spectra. Results for *i*-Ag-In-Yb are from the fivefold surface after annealing. Results for *i*-Cd-Yb are taken from Ref. 17. The separation of bulk doublets ΔE_B, surface doublets ΔE_S and surface core-level shift $\Delta E_{SCLS}(=\mathrm{BE}_{4f^S_{7/2}}-\mathrm{BE}_{4f^B_{7/2}})$ are also presented.

	$f^B_{7/2}$	$f^B_{5/2}$	$f^S_{7/2}$	$f^S_{5/2}$	ΔE_B	ΔE_S	ΔE_{SCLS}
i-Ag-In-Yb	0.68	1.90	1.18	2.50	1.22	1.32	0.50
Pure Yb	1.25	2.50	1.75	3.00	1.25	1.25	0.50
i-Cd-Yb	0.70	2.00	1.08	2.37	1.30	1.29	0.36

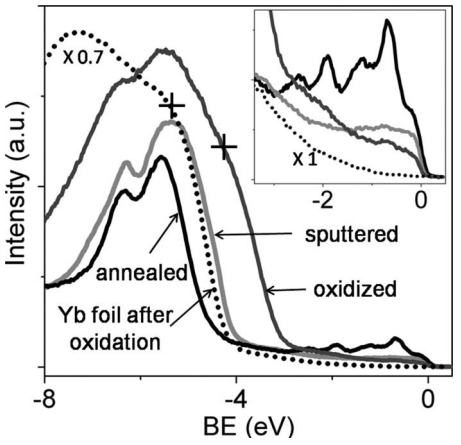

FIG. 4. He-I valence band spectra of the fivefold *i*-Ag-In-Yb surface after sputtering, annealing, and oxidation. Valence band spectrum of pure Yb after oxidation is also given for comparison (dotted line, intensity is scaled by a factor of 0.7). The intensity of each spectrum is subtracted from the background intensity above the Fermi level. The + symbol marks a shoulder developed due to oxidation. The inset shows a closeup near the Fermi level.

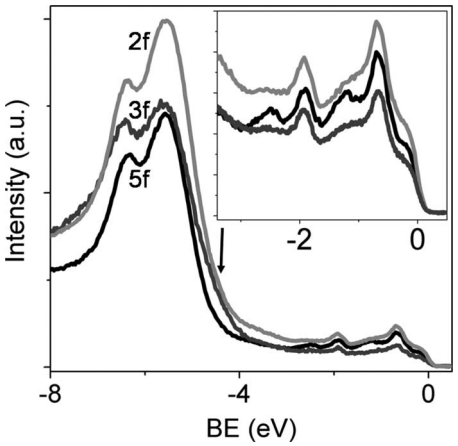

FIG. 5. He-I valence band spectra of the fivefold, threefold, and twofold surfaces of *i*-Ag-In-Yb after annealing. The intensity of each spectrum is subtracted from the background intensity above the Fermi level. The inset shows a closeup near the Fermi level. The arrow indicates a shoulder which develops due to surface contamination.

finite Fermi edge is still observable in the UPS spectra from the quasicrystal unlike in pure Yb which shows no Fermi edge after oxidation (Fig. 4 inset). The shift of Yb 4*f* band to higher binding energy is due to the formation of ytterbium oxide, i.e., charge transfer from Yb to oxygen increases the Coulombic interaction of 4*f* electrons with the positive ions. Such a charge transfer is verified by XPS measurements and it is also in accordance with work-function results.

XPS was used to check the influence of oxygen exposure from sub-Langmuir to several hundreds of Langmuirs on the Ag-, In-, and Yb-derived bands in *i*-Ag-In-Yb. At the selected exposure of 10 L, the Ag band was unchanged, In band is also almost not influenced but oxidation of Yb is saturated and additional peaks are observed in the Yb 4*d* spectra at higher binding energies (not shown), in agreement with UPS results. A finite Fermi edge observed after oxidation is thus considered to be due to contributions from In and Ag, which is expected from calculations as explained above.

Now we compare the valence band spectra taken from three high-symmetry surfaces of *i*-Ag-In-Yb. As for the fivefold surface, the threefold, and twofold surfaces were studied by UPS after sputtering, annealing, and oxidation. The chemical composition of the threefold and twofold surfaces after sputtering analyzed by XPS is found to be comparable to that of the fivefold surface. The surfaces after annealing regain the bulk composition and yield fairly large atomically flat terraces in STM (not shown). Both Fourier transforms of STM images and LEED patterns from the surfaces reveal the long-range order expected from the bulk.

Figure 5 shows UPS spectra taken from the fivefold, threefold, and twofold surfaces after annealing. The Ag 4*d*, Yb $4f^B_{7/2}$, and Yb $4f^B_{5/2}$ peaks observed in the fivefold surface are reproduced at the identical positions in the twofold and threefold surfaces. The Yb $4f^S_{7/2}$ and $4f^S_{5/2}$ peaks are also observed at almost the same positions (implying an identical surface core-level shift in all three surfaces) but these peaks are more pronounced in the fivefold surface than in other two surfaces. This is probably due to contamination of the other two surfaces during UPS measurements. The threefold surface is very reactive such that the Yb $4f^S_{7/2}$ and Yb $4f^S_{5/2}$ peaks start to deteriorate within a few minutes after a clean surface is obtained due to surface contamination by the residual gases in the UHV chamber. A shoulder observed at around 4.5 eV (indicated by an arrow in Fig. 5) is further evidence of surface contamination. UPS spectra from the threefold and twofold surfaces after sputtering show changes which are similar to those observed in the fivefold surface. The same is true for the surfaces after oxidation.

The work function (ϕ) of a solid is generally modified by the change in the surface in terms of, for example, morphology, orientation, and adsorption. In order to verify this phenomenon in the quasicrystalline system, we measured the work function of the fivefold, threefold, and twofold surfaces after different treatments: sputtering, annealing, and oxidation. The work function is obtained from the width of a UPS spectrum, which is given by $W=h\nu-\phi$, $h\nu$ being the energy of the incident He-I radiation. A −10 V bias is applied to the sample during UPS measurements in order to detect the slowest photoelectrons which have barely enough energy to overcome the work function of the sample. This yields a sharp slope at the low-energy edge (the secondary cutoff) (Fig. 6). The results of work-function measurements are presented in Table III. The work functions of pure Ag, In, and Yb were also measured and are presented in the same table for comparison. The measured values for pure metals are consistent with previous results.[37] Oxygen exposure of all surfaces was the same (10 L). At this exposure, pure Ag and In are not influenced as mentioned above and thus the work function after oxygen exposure remains unchanged. For *i*-Ag-In-Yb, the work function is almost not influenced by surface orientation, but increases after sputtering or oxidation.

The work function of a $Ag_xIn_yYb_{1-x-y}$ alloy estimated by a linear interpolation of work functions of pure metals would

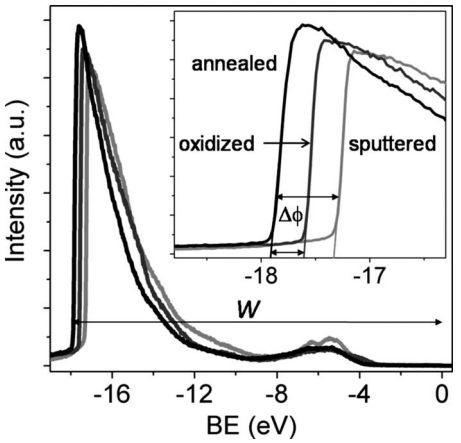

FIG. 6. He-I valence band spectra of the fivefold *i*-Ag-In-Yb surface after sputtering, annealing, and oxidation with a −10 V bias applied to the sample. The inset shows a closeup of the secondary cutoff. The shift of the secondary cutoff ($\Delta\phi$) to lower binding energy manifests an increase in work function, i.e., decrease in width of the spectrum, $W=h\nu-\phi$.

be $x\phi_{\mathrm{Ag}}+y\phi_{\mathrm{In}}+(1-x-y)\phi_{\mathrm{Yb}}$, ϕ_M (M=Ag, In, or Yb) being the work function of pure metals. The linear interpolation for the annealed surface is ~4 eV; which is higher than the measured value. This is not unusual, however, the work function of other alloys was also found to be lower than linear interpolation.[38] Based on the linear interpolation, one would expect an increase in work function after sputtering because of Ag enrichment in the surface region as Ag has a higher work function than In and Yb. This has indeed been observed: the work function is increased by 0.3–0.5 eV after sputtering (see Table III). The work function also increases after oxidation because the charge transfer from the surface Yb atoms to oxygen adsorbates forms a dipole layer parallel to the dipole layer of the clean surface, which opposes the ejection of electrons from the sample.

V. SUMMARY AND CONCLUSIONS

We have investigated the valence band structure of the icosahedral *i*-Ag-In-Yb quasicrystal. UPS was employed to study the fivefold, threefold, and twofold surfaces (all possible high-symmetry surfaces) after sputtering, annealing, and oxidation. The observed valence band was compared with that of pure Ag, In, and Yb as well as with electronic-structure calculations of the 1/1 approximant of *i*-Ag-In-Yb.

TABLE III. Work function of various samples after different surface treatments measured from the width of UPS spectrum.

	Sputtered (eV)	Annealed (eV)	Oxidized (eV)
Pure Ag	4.6		4.6
Pure In	4.1		4.1
Pure Yb	2.6		3.1[a]
Fivefold *i*-Ag-In-Yb	3.8	3.3	3.6
Threefold *i*-Ag-In-Yb	3.6	3.3	3.5
Twofold *i*-Ag-In-Yb	3.8	3.3	3.5

[a]Taken from Ref. 36.

UPS reveals that the valence band near the Fermi level is dominated by Yb 4*f*-derived states, in agreement with the calculated results. Surface core-level-shifted components are identified in all three surfaces after annealing. The magnitude of the shift is similar to that of pure Yb. The observed valence band features are found to be very similar to those observed for *i*-Cd-Yb quasicrystal. Differences noticed in the surface-induced features are thought to be related to surface preparation methods. Consistent with Cd-Yb results, calculations reveal a pseudogap in the density of states due to a hybridization of the Yb 5*d* band with the Ag 5*p* and In 5*p* bands.

The valence band is modified after sputtering and oxidation. The Yb 4*f* band diminishes after sputtering possibly due to the depletion of Yb in the surface region, while oxidation shifts the Yb 4*f* band to higher binding energy due to charge transfer from Yb to oxygen. The influence of surface modifications and surface orientation on the work function was also studied. The work function after sputtering is increased by 0.3–0.5 eV, which is interpreted in terms of Ag enrichment in the surface region that occurs after sputtering. Oxidation also increases the work function due to a charge transfer from Yb atoms to oxygen adsorbates. The work function was found to be almost independent of the surface orientation.

ACKNOWLEDGMENTS

This work was supported by the U.K. Engineering and Physical Sciences Research Council (EPSRC) under Grants No. EP/D071828/1 and No. EP/D05253X/1). G.S. is grateful to EPSRC for funding under VBP scheme. We would like to thank J. A. Smerdon for a critical reading of the manuscript.

*Corresponding author; h.r.sharma@liv.ac.uk

[1] A. P. Tsai, J. Q. Guo, E. Abe, H. Takakura, and T. J. Sato, Nature (London) **408**, 537 (2000).
[2] H. Takakura, C. P. Gomez, A. Yamamoto, M. de Boissieu, and A. P. Tsai, Nature Mater. **6**, 58 (2007).
[3] Y. Ishii and T. Fujiwara, Phys. Rev. Lett. **87**, 206408 (2001).
[4] Z. Stadnik, *Quasicrystals: Structure and Physical Properties* (Wiley, New York, 2003).
[5] G. T. de Laissardière, D. Nguyen-Manh, and D. Mayou, Prog. Mater. Sci. **50**, 679 (2005).
[6] R. Tamura, T. Takeuchi, C. Aoki, S. Takeuchi, T. Kiss, T. Yokoya, and S. Shin, Phys. Rev. Lett. **92**, 146402 (2004).
[7] A. L. Pope, T. M. Tritta, R. Gagnon, and J. Strom-Olsen, Appl. Phys. Lett. **79**, 2345 (2001).

[8] Y. Muro, T. Sasakawa, T. Sumemitsu, T. Takabatake, R. Tamurai, and S. Takeuchi, Jpn. J. Appl. Phys. **41**, 3787 (2002).
[9] R. Tamura, Y. Murao, S. Takeuchi, K. Tokiwa, T. Watanabe, T. J. Sato, and A. P. Tsai, Jpn. J. Appl. Phys., Part 2 **40**, L912 (2001).
[10] H. R. Sharma, M. Shimoda, and A. P. Tsai, Adv. Phys. **56**, 403 (2007), references therein.
[11] V. Fournée and P. A. Thiel, J. Phys. D **38**, R83 (2005).
[12] J. Q. Guo and A. P. Tsai, Philos. Mag. Lett. **82**, 349 (2002).
[13] S. Ohhashi, J. Hasegawa, S. Takeuchi, and A. P. Tsai, Philos. Mag. **87**, 3089 (2007).
[14] H. R. Sharma, M. Shimoda, S. Ohhashi, and A. P. Tsai, Philos. Mag. **87**, 2989 (2007).
[15] H. R. Sharma, M. Shimoda, K. Sagisaka, H. Takakura, J. A. Smerdon, P. J. Nugent, R. McGrath, D. Fujita, S. Ohhashi, and A. P. Tsai, Phys. Rev. B **80**, 121401(R) (2009).
[16] Y. K. Kuo, K. M. Sivakumar, H. H. Lai, C. N. Ku, S. T. Lin, and A. B. Kaiser, Phys. Rev. B **72**, 054202 (2005).
[17] R. Tamura, Y. Murao, S. Takeuchi, T. Kiss, T. Yokoya, and S. Shin, Phys. Rev. B **65**, 224207 (2002).
[18] C. Cui and A. P. Tsai, J. Cryst. Growth **312**, 131 (2010).
[19] C. P. Goméz (private communication).
[20] A. Palenzona, J. Less-Common Met. **25**, 367 (1971).
[21] G. Kresse and J. Hafner, Phys. Rev. B **47**, 558 (1993).
[22] G. Kresse and J. Furthmüller, Phys. Rev. B **54**, 11169 (1996).
[23] G. Kresse and D. Joubert, Phys. Rev. B **59**, 1758 (1999).
[24] *International Tables for Crystallography*, Vol. A, edited by Th. Hahn (Kluwer, Dordrecht, 2002).
[25] O. K. Andersen, O. Jepsen, and D. Glötzel, in *Highlights in Condensed Matter Theory*, edited by F. Bassani, F. Fumi, and M. P. Tosi (North-Holland, Amsterdam, 1985).
[26] B. Johansson and N. Mårtensson, Phys. Rev. B **21**, 4427 (1980).
[27] F. Gerken, A. S. Flodstrom, J. Barth, L. I. Johansson, and C. Kunz, Phys. Scr. **32**, 43 (1985).
[28] E. J. Cho *et al.*, Phys. Rev. B **47**, 3933 (1993).
[29] M. Bodenbach, A. Höhr, C. Laubschat, G. Kaindl, and M. Methfessel, Phys. Rev. B **50**, 14446 (1994).
[30] F. Müller and K. Stöwe, Z. Anorg. Allg. Chem. **629**, 1805 (2003).
[31] A. Svane, N. E. Christensen, L. Petit, Z. Szotek, and W. M. Temmerman, Phys. Rev. B **74**, 165204 (2006).
[32] A. I. Boronin, S. V. Koscheev, and G. M. Zhidomirov, J. Electron Spectrosc. Relat. Phenom. **96**, 43 (1998).
[33] P. Ebert, M. Feuerbacher, N. Tamura, M. Wollgarten, and K. Urban, Phys. Rev. Lett. **77**, 3827 (1996).
[34] V. Fournée, P. J. Pinhero, J. W. Anderegg, T. A. Lograsso, A. R. Ross, P. C. Canfield, I. R. Fisher, and P. A. Thiel, Phys. Rev. B **62**, 14049 (2000).
[35] B. D. Padalia, W. C. Lang, P. R. Norris, L. M. Watson, and D. J. Fabian, Proc. R. Soc. London, Ser. A **354**, 269 (1977).
[36] E. Bertel, G. Strasser, F. P. Netzer, and J. A. D. Matthew, Surf. Sci. **118**, 387 (1982).
[37] J. Hölzl, F. K. Schulte, and H. Wagner, in *Solid Surface Physics*, edited by G. Höhler (Springer-Verlag, Berlin, 1979).
[38] R. Ishii, K. Matsumura, A. Sakai, and T. Sakata, Appl. Surf. Sci. **169-170**, 658 (2001).